ARTICLE IN PRESS

Foot and Ankle Surgery xxx (xxxx) xxx–xxx

Contents lists available at ScienceDirect

Foot and Ankle Surgery

journal homepage: www.journals.elsevier.com/foot-and-ankle-surgery

Biomechanical effects of selective tarsometatarsal arthrodesis configurations: A finite element analysis

Fatih Barça [a,*,1], Ekin Barış Demir [a,2], Musa Güngörürler [b,3], Burak Menderes Akdoğan [c,4], Çağrı Havıtçıoğlu [d,5], Mutlu Akdoğan [a,6], Yalım Ateş [a,7], Halis Atıl Atilla [a,8]

[a] Ankara Etlik City Hospital, Department of Orthopaedics and Traumatology, Ankara, Turkey
[b] Department of Biomechanics, Institute of Health Sciences, Dokuz Eylul University, Izmir, Turkey
[c] Rize State Hospital, Department of Orthopaedics and Traumatology, Rize, Turkey
[d] Near East University Faculty of Medicine, Department of Orthopaedics and Traumatology, Nicosia, Cyprus

ARTICLE INFO

Article history:
Received 6 January 2026
Received in revised form 5 February 2026
Accepted 23 February 2026

Keywords:
Fusion
Computational
Lisfranc injury
Lapidus
Pressure
Joint reaction force
Adjacent joint biomechanics

ABSTRACT

Background: The biomechanical effects of different tarsometatarsal (TMT) arthrodesis configurations on adjacent joints remain unclear. This finite element study evaluated load transfer and pressure redistribution following selective TMT fusion.
Methods: Six TMT arthrodesis configurations, from isolated first TMT fusion to constructs including the third TMT joint, were analyzed. Joint reaction forces, plantar pressure, and tibiotalar contact pressure were assessed relative to an intact model across stance phases.
Results: Arthrodesis altered midfoot joint reaction forces, while total tibiotalar forces remained largely unchanged. The medial - intermediate intercuneiform and calcaneocuboid joints showed the greatest increases, particularly with inclusion of the third TMT joint. Plantar pressure increased mainly in the first and second metatarsal regions, and tibiotalar contact pressure redistributed along an anterolateral - posteromedial axis.
Conclusion: TMT arthrodesis alters foot biomechanics in a configuration-dependent manner. Extension to the third TMT joint produced the greatest biomechanical alterations.
Level of evidence: V, computational biomechanical study

1. Introduction

The tarsometatarsal (TMT) joint complex connects the midfoot to the forefoot and consists of joints formed by the bases of the metatarsals with the cuneiform and cuboid bones. The lateral portion of TMT joint complex exhibits relatively greater mobility and functions as a shock absorber, whereas the medial and middle columns are comparatively rigid [1]. The rigidity of medial and middle columns is critical for normal foot biomechanics and for maintaining transverse arch stability [2].

Since the early 1900s, medial column hypermobility has been implicated in the pathogenesis of hallux valgus, leading to the widespread adoption of first tarsometatarsal (TMT) arthrodesis following the work of Lapidus [3,4]. To improve construct stability and reduce complications, extension of the fusion to the second metatarsal and intercuneiform joints has been advocated [4–7], although its necessity remains controversial.

* Correspondence to: Ankara Etlik Şehir Hastanesi, Varlık Mah., Halil Sezai Erkut Cd. Yenimahalle, Ankara 06170, Turkey.
E-mail addresses: fatihbarca@hotmail.com (F. Barça), ekinbarisdemir@hotmail.com (E.B. Demir), musagngrrlr@gmail.com (M. Güngörürler), menderesburak@gmail.com (B.M. Akdoğan), drcagrihavitcioglu@gmail.com (Ç. Havıtçıoğlu), mutluakdogan@yahoo.com (M. Akdoğan), dryalimates@msn.com (Y. Ateş), dratilatilla@hotmail.com (H.A. Atilla).
[1] ORCID: 0000-0002-8167-6146
[2] ORCID: 0000-0002-9986-1905
[3] ORCID: 0000-0002-5137-6919
[4] ORCID: 0000-0001-9403-2369
[5] ORCID: 0009-0008-6761-5225
[6] ORCID: 0000-0001-8419-4065
[7] ORCID: 0000-0002-4158-1054
[8] ORCID: 0000-0002-5670-1469

https://doi.org/10.1016/j.fas.2026.02.005
1268-7731/

Please cite this article as: F. Barça, E.B. Demir, M. Güngörürler et al., Biomechanical effects of selective tarsometatarsal arthrodesis configurations: A finite element analysis, Foot and Ankle Surgery, https://doi.org/10.1016/j.fas.2026.02.005

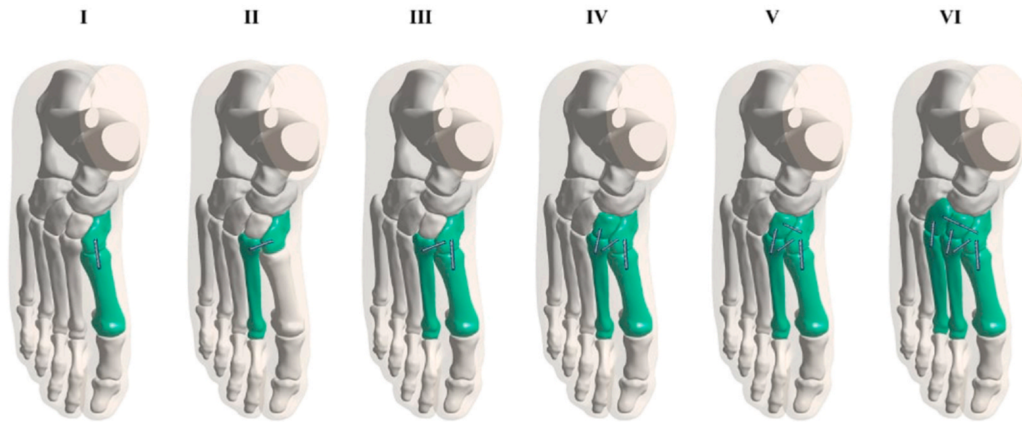

Fig. 1. Midfoot arthrodesis models. Model I: First TMT joint. Model II: Medial cuneiform - second metatarsal joint. Model III: Combination of Model I and Model II. Model IV: Addition of second TMT joint to model III. Model V: Addition of medial-intermediate cuneiform joint to model IV. Model VI: Addition of third TMT joint to Model V.

Similarly, medial column TMT arthrodesis is increasingly used in the treatment of Lisfranc injuries, where primary arthrodesis has been shown to provide clinical outcomes and return-to-sport rates comparable or superior to internal fixation [8–10]. Despite its frequent use, the biomechanical consequences of extending medial column fusion to adjacent joints remain incompletely understood.

Adjacent joint arthritis is a well-recognized complication of arthrodesis, particularly involving the tibiotalar and subtalar joints [11–15]. This has been attributed to altered load transfer and increased mechanical stress in adjacent joints following fusion [16]. However, biomechanical data specifically addressing adjacent joint loading after tarsometatarsal arthrodesis remain limited [17–20]. In addition to changes in joint loading, alterations in plantar pressure distribution represent an important and clinically relevant manifestation of load redistribution following arthrodesis.

Because direct assessment of joint loading after arthrodesis is limited in clinical settings, finite element analysis has been used to investigate the biomechanical effects of tarsometatarsal fusion. Existing finite element analysis studies have mainly focused on fixation constructs [21–23] or combined first and second TMT arthrodesis [20], providing limited insight into how selective medial and middle column fusions affect adjacent joints and plantar pressure. Therefore, this study aimed to evaluate changes in joint reaction forces, plantar pressure distribution, and tibiotalar contact pressure across different phases of gait following selective TMT arthrodesis configurations.

2. Materials and methods

2.1. Study design

This study used a subject-specific finite element (FE) model to evaluate the biomechanical effects of selective tarsometatarsal (TMT) arthrodesis configurations on adjacent joint loading, plantar pressure distribution, and tibiotalar contact pressure during gait.

2.2. Development of finite element model

A three-dimensional FE model of the right foot and ankle was generated from computed tomography data of a healthy adult male (33 years, 80 kg) with no history of foot or ankle pathology. Bone geometries were segmented and reconstructed to include the tibia, fibula, hindfoot, midfoot, forefoot, and phalanges. A neutral anatomical alignment was established based on standardized joint coordinate system definitions.

Ligaments were modeled as tension-only elements, and articular cartilage and encapsulated soft tissue were incorporated to allow physiologic joint motion. All materials were assumed to be homogeneous, isotropic, and linearly elastic, consistent with commonly used foot and ankle FE models [24–47]. Detailed material properties, ligament definitions, and mesh characteristics are provided in the Supplementary Material.

2.3. Midfoot arthrodesis models (Fig. 1)

In the finite element analyses, the intact model was evaluated first and served as the reference condition. Subsequently, six arthrodesis configurations (Models I - VI) were generated to represent commonly used clinical fusion strategies. Arthrodesis was simulated by removing the articular cartilage at the corresponding joints, assigning bone material properties to the joint interfaces, and applying bonded contact conditions between the fused surfaces. This approach eliminated relative motion at the fused joints while preserving load transfer across the fusion sites. No fixation hardware was modeled in order to isolate the biomechanical effects of joint fusion itself.

In Model I, fusion was applied solely to the first tarsometatarsal (TMT) joint. Model II represented isolated fusion of the medial cuneiform - second metatarsal joint. Model III combined these two fusions. In Model IV, fusion of the second TMT joint was added to Model III. Model V further included fusion of the medial - intermediate intercuneiform joint. In the final configuration (Model VI), fusion of the third TMT joint and the intermediate - lateral intercuneiform joint was added, resulting in the most extensive fusion construct (Fig. 1).

2.4. Boundary and loading conditions

Physiologic loading conditions corresponding to normal walking were applied. Ground reaction forces and major muscle forces were obtained from a validated musculoskeletal gait model [28] and applied to the FE model. Three representative phases of stance - early stance, midstance, and late stance - were analyzed.

The proximal tibia and fibula were fully constrained. Ground contact was modeled with friction, allowing force transmission to the plantar surface. Identical boundary and loading conditions were applied to the intact and all arthrodesis models to enable direct comparison (see Supplementary Material).

2.5. Outcome measures

For each arthrodesis configuration and gait phase, the following outcomes were evaluated and compared with the intact model: Joint reaction forces (JRFs) at 17 selected foot and ankle joints, plantar

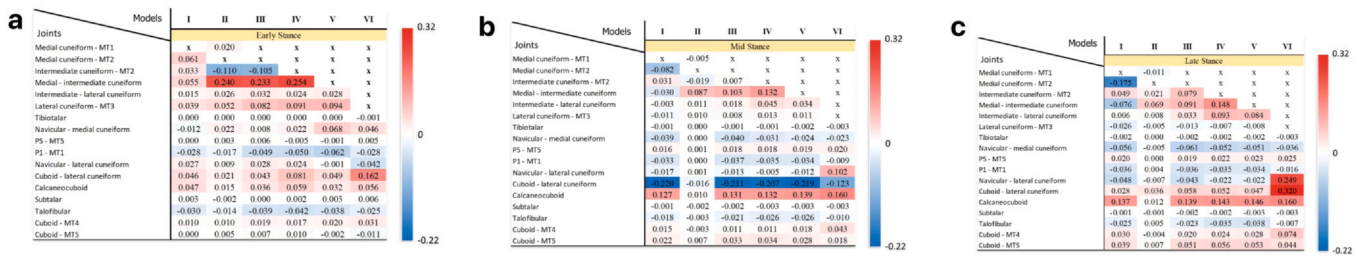

a Early Stance

Joints \ Models	I	II	III	IV	V	VI
Medial cuneiform - MT1	x	0.020	x	x	x	x
Medial cuneiform - MT2	0.061	x	x	x	x	x
Intermediate cuneiform - MT2	0.033	-0.110	-0.105	x	x	x
Medial - intermediate cuneiform	0.055	0.240	0.233	0.254	x	x
Intermediate - lateral cuneiform	0.015	0.026	0.032	0.024	0.028	x
Lateral cuneiform - MT3	0.039	0.052	0.082	0.091	0.094	x
Tibiotalar	0.000	0.000	0.000	0.000	0.000	-0.001
Navicular - medial cuneiform	-0.012	0.022	0.008	0.022	0.068	0.046
P5 - MT5	0.000	0.003	0.006	-0.005	-0.001	0.005
P1 - MT1	-0.028	-0.017	-0.049	-0.050	-0.062	-0.028
Navicular - lateral cuneiform	0.027	0.009	0.028	0.024	-0.001	-0.042
Cuboid - lateral cuneiform	0.046	0.021	0.043	0.081	0.049	0.162
Calcaneocuboid	0.047	0.015	0.036	0.059	0.032	0.056
Subtalar	0.003	-0.002	0.000	0.002	0.003	0.006
Talofibular	-0.030	-0.014	-0.039	-0.042	-0.038	-0.025
Cuboid - MT4	0.010	0.010	0.019	0.017	0.020	0.031
Cuboid - MT5	0.000	0.005	0.007	0.010	-0.002	-0.011

b Mid Stance

Joints \ Models	I	II	III	IV	V	VI
Medial cuneiform - MT1	x	-0.005	x	x	x	x
Medial cuneiform - MT2	-0.082	x	x	x	x	x
Intermediate cuneiform - MT2	0.031	-0.019	0.007	x	x	x
Medial - intermediate cuneiform	-0.030	0.087	0.103	0.132	x	x
Intermediate - lateral cuneiform	-0.003	0.011	0.018	0.045	0.034	x
Lateral cuneiform - MT3	-0.011	0.010	0.008	0.013	0.011	x
Tibiotalar	-0.001	0.000	-0.001	-0.001	-0.002	-0.003
Navicular - medial cuneiform	-0.039	0.000	-0.040	-0.031	-0.024	-0.023
P5 - MT5	0.016	0.001	0.018	0.018	0.019	0.020
P1 - MT1	-0.033	0.000	-0.037	-0.035	-0.034	-0.009
Navicular - lateral cuneiform	-0.017	0.001	-0.013	-0.005	-0.012	0.102
Cuboid - lateral cuneiform	-0.220	-0.016	-0.211	-0.207	-0.219	-0.123
Calcaneocuboid	0.127	0.010	0.131	0.132	0.139	0.160
Subtalar	-0.001	-0.002	-0.002	-0.003	-0.003	-0.003
Talofibular	-0.018	-0.003	-0.021	-0.026	-0.026	-0.010
Cuboid - MT4	0.015	-0.003	0.011	0.011	0.018	0.043
Cuboid - MT5	0.022	0.007	0.033	0.034	0.028	0.018

c Late Stance

Joints \ Models	I	II	III	IV	V	VI
Medial cuneiform - MT1	x	-0.011	x	x	x	x
Medial cuneiform - MT2	-0.175	x	x	x	x	x
Intermediate cuneiform - MT2	0.049	0.021	0.079	x	x	x
Medial - intermediate cuneiform	-0.076	0.069	0.091	0.148	x	x
Intermediate - lateral cuneiform	0.006	0.008	0.033	0.093	0.084	x
Lateral cuneiform - MT3	-0.026	-0.005	-0.013	-0.007	-0.008	x
Tibiotalar	-0.002	0.000	-0.002	-0.002	-0.002	-0.003
Navicular - medial cuneiform	-0.056	-0.005	-0.061	-0.052	-0.051	-0.036
P5 - MT5	0.020	0.000	0.019	0.022	0.023	0.025
P1 - MT1	-0.036	0.004	-0.036	-0.035	-0.034	-0.016
Navicular - lateral cuneiform	-0.048	-0.007	-0.043	-0.022	-0.022	0.249
Cuboid - lateral cuneiform	0.028	0.036	0.058	0.052	0.047	0.320
Calcaneocuboid	0.137	0.012	0.139	0.143	0.146	0.160
Subtalar	-0.001	-0.001	-0.002	-0.002	-0.003	-0.003
Talofibular	-0.025	0.005	-0.023	-0.035	-0.038	-0.007
Cuboid - MT4	0.030	-0.004	0.020	0.024	0.028	0.074
Cuboid - MT5	0.039	0.007	0.051	0.056	0.053	0.044

Fig. 2. Joint reaction force comparisons relative to the intact model. (a) Early stance. (b) Midstance. (c) Late stance.

pressure distribution and contact pressure distribution at the tibiotalar joint. Differences were quantified to assess changes in load transfer and pressure redistribution associated with each fusion strategy.

2.6. Model credibility

Model behavior was qualitatively compared with previously published experimental and computational studies evaluating plantar pressure distribution and ankle joint mechanics, demonstrating consistency in both the magnitude and spatial distribution of results [24,25,29,30]. This comparison was used to support the biomechanical credibility of the model.

2.7. Software

All simulations were performed using a commercial finite element solver (ANSYS Workbench 2021 R2; ANSYS Inc., Canonsburg, PA, USA). Additional details regarding meshing strategy, convergence assessment, and material assignments are provided in the Supplementary Material.

3. Results

The intact model served as the reference condition for all biomechanical comparisons.

3.1. Joint reaction force alterations (Fig. 2)

Across all gait phases, joint reaction force (JRF) alterations were predominantly observed within the midfoot in all models. The medial - intermediate intercuneiform and calcaneocuboid joints demonstrated the most pronounced increases in JRF. Forces at the tibiotalar and subtalar joints remained largely unchanged (generally < 5% deviation from the intact condition).

Isolated medial cuneiform - second metatarsal fusion (Model II) consistently produced the smallest deviations from the intact condition, with JRF changes remaining below 10% across all evaluated joints and gait phases. In contrast, inclusion of the third tarsometatarsal (TMT) joint (Model VI) resulted in the greatest alterations, with increases in JRF reaching approximately 25–32% at the calcaneocuboid and lateral column joints, particularly during late stance. Intermediate configurations (Models III - V) demonstrated comparable JRF patterns, with differences between these models generally remaining below 5% (Fig. 2).

3.2. Plantar pressure distribution changes (Fig. 3)

Relative to the intact model, plantar pressure increases were predominantly observed in the first and second metatarsal regions across most arthrodesis configurations. These changes were phase dependent and most pronounced during late stance.

Model II showed minimal deviation from the intact plantar pressure pattern, with peak pressure changes generally remaining below 10–15 kPa across all gait phases. In contrast, Model VI demonstrated the largest plantar pressure alterations, reaching approximately 25–30 kPa during midstance and up to 50–60 kPa during late stance. Models III, IV, and V exhibited highly similar plantar pressure distributions, with inter-model differences remaining small compared with those observed in Model VI (Fig. 3).

3.3. Tibiotalar contact pressure redistribution (Fig. 4)

Total tibiotalar joint reaction forces did not change substantially following tarsometatarsal arthrodesis; however, a consistent redistribution of tibiotalar contact pressure was observed across all arthrodesis models. Pressure alterations followed a characteristic anterolateral - posteromedial pattern on the talar articular surface throughout the stance phase.

The magnitude of tibiotalar pressure redistribution increased with the extent of fusion. Model II demonstrated the smallest changes, whereas Model VI exhibited the greatest alterations, with peak contact pressure differences reaching approximately 300–350 kPa during midstance and up to 500–550 kPa during late stance (Fig. 4).

4. Discussion

The most important finding of the present study is that the biomechanical consequences of tarsometatarsal arthrodesis strongly depend on the extent of fusion. While isolated medial cuneiform - second metatarsal fusion resulted in minimal alterations in joint reaction forces, plantar pressure, and tibiotalar contact mechanics, extension of fusion to the third tarsometatarsal joint produced pronounced changes, particularly involving the lateral column and adjacent joints. Among these, the calcaneocuboid joint consistently demonstrated increased joint reaction forces, highlighting its susceptibility to load redistribution following more extensive fusion constructs. Notably, although total tibiotalar joint reaction forces remained largely unchanged, a consistent redistribution of contact pressure along an anterolateral - posteromedial axis was observed, with increasing magnitude as the fusion construct was extended. These findings suggest that selective fusion strategies may substantially influence load transfer patterns beyond the fused joints.

TMT joint arthrodesis is commonly employed in the treatment of various forefoot and midfoot pathologies. The first TMT joint arthrodesis (Model I), popularized by Lapidus, is widely used in the surgical management of advanced hallux valgus [4]. In selected cases, fusion may be extended to additional medial column articulations to enhance construct stability or address midfoot instability [5,6]. Isolated fixation between the medial cuneiform and the second metatarsal represents a treatment option, particularly for ligamentous Lisfranc injuries (Model II) [31]. Furthermore, arthrodesis of the third TMT joint should be considered in degenerative conditions

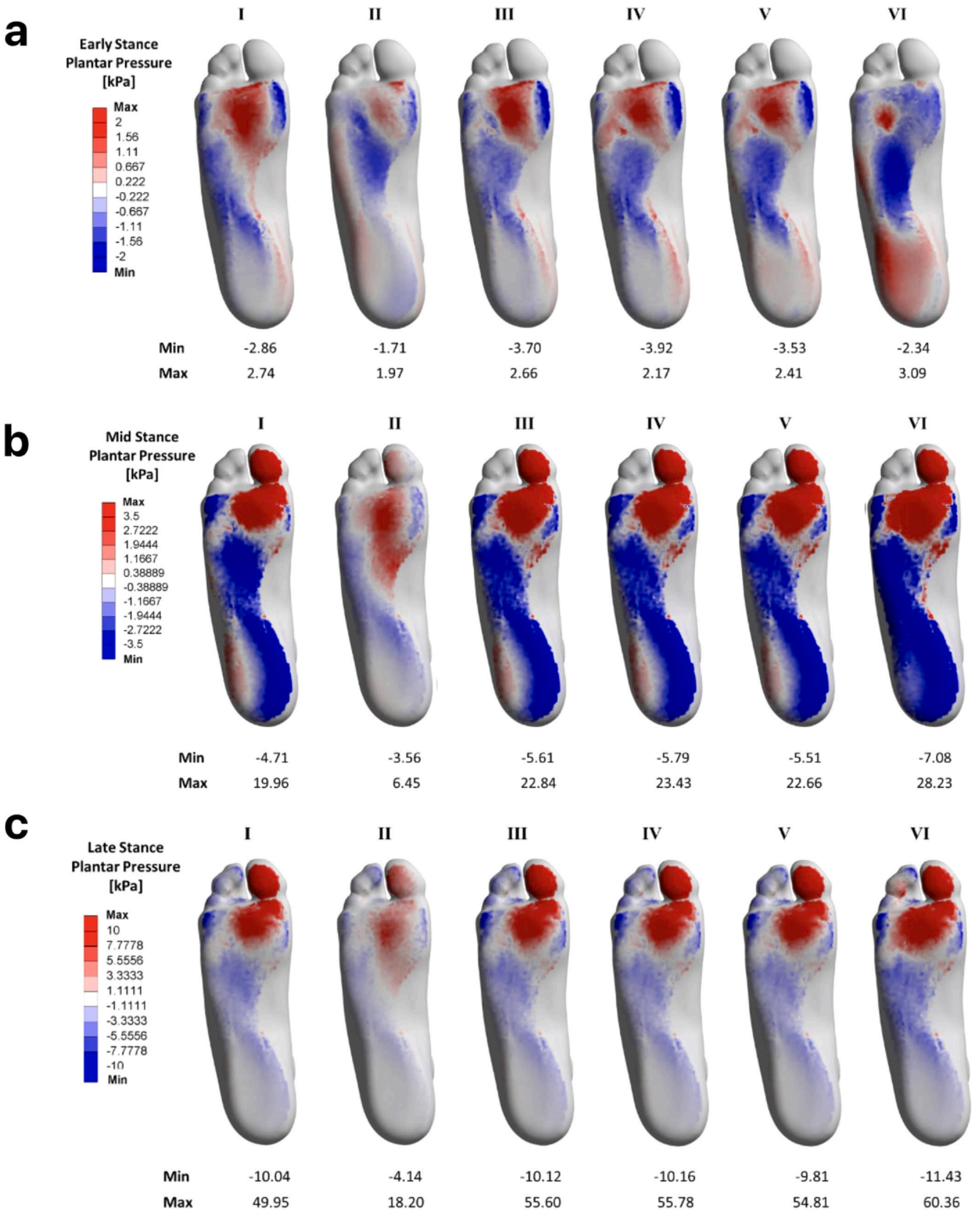

Fig. 3. Plantar pressure distribution comparisons relative to the intact model. (a) Early stance. (b) Midstance. (c) Late stance.

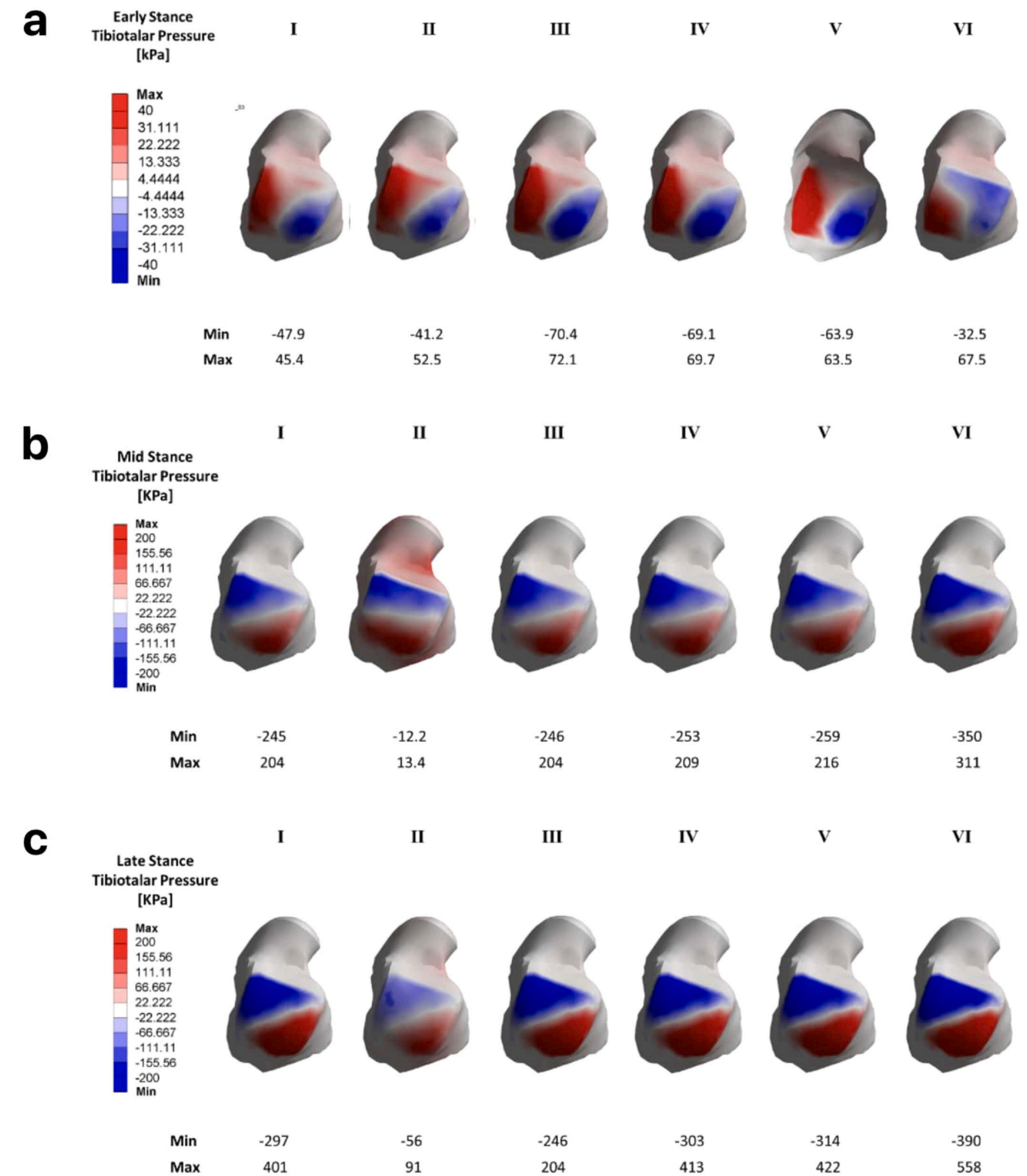

Fig. 4. Tibiotalar contact pressure distribution comparisons relative to the intact model. (a) Early stance. (b) Midstance. (c) Late stance.

[32] or following Lisfranc injuries [25] (Model VI). Collectively, the arthrodesis configurations evaluated in this study span a range of fusion extents and were included to provide a structured biomechanical framework for assessing the biomechanical effects of incremental midfoot fusion on load transfer and adjacent joint mechanics.

Joint reaction force (JRF) is the vectoral sum of all the forces acting on a joint, and increase in JRF can be considered as a key factor in osteoarthritis pathogenesis [33]. Although there are no established cut-off points for alterations in JRF in terms of clinical relevance, the investigation of changes in this study implicates several findings. One of the main findings is that without fusion of medial-intermediate intercuneiform joint, there was a constant increase of JRF on this joint. Intercuneiform joint issues, especially instability, was emphasized in hallux valgus [34,35], and adding a fusion of this joint to the construct was recommended to avoid potential complications related to this joint [35]. The present findings biomechanically support consideration of intercuneiform fusion in selected cases by demonstrating increased joint loading when this joint remains unfused.

The calcaneocuboid joint is a key component of the transverse tarsal joint complex and plays a critical role in maintaining the lateral longitudinal arch. Although isolated pathology of this joint is relatively uncommon, it has been previously reported that calcaneocuboid joint arthritis may progress to tibiotalar joint arthritis and contribute to chronic pain over the long term [36]. In this context, the present findings demonstrate increased loading of the calcaneocuboid joint following more extensive TMT arthrodesis, suggesting a potential biomechanical mechanism by which adjacent joint degeneration may be promoted. Nevertheless, the clinical implications of this altered loading pattern require confirmation in future clinical studies.

The total JRF at the tibiotalar joint did not change substantially across any arthrodesis model. However, analysis of contact pressure distribution revealed a consistent shift in pressure toward an anterolateral - posteromedial direction in nearly all models. This redistribution was minimal in Model II (isolated medial cuneiform - second metatarsal fusion) and tended to increase with the number of fused joints, reaching its greatest magnitude in Model VI across all phases of gait. Previous biomechanical studies investigating ankle fractures or malalignment have demonstrated marked alterations in tibiotalar contact pressures [30,37,38]. Although the magnitude of pressure change observed in the present study was quantitatively smaller than that reported in fracture models (maximum 558 kPa during late stance in Model VI), we believe that these alterations may nonetheless have clinical relevance. While no definitive threshold for clinically significant tibiotalar pressure changes has been established, even subtle modifications in cartilage load transfer may predispose to secondary pathological processes, including cartilage degeneration and the development of ankle arthritis.

We found that inclusion of the third TMT joint in the fusion construct, particularly affecting the lateral column joints (calcaneocuboid and cuboid - lateral cuneiform), resulted in increased JRF and exerted the greatest influence on both tibiotalar joint loading and plantar pressure distribution. Although incorporation of the third TMT joint may be necessary in certain clinical scenarios, particularly following Lisfranc injuries, it is not routinely included in fusion constructs except in cases of isolated pathology such as fracture or degenerative arthritis. In a cadaveric study, Kim et al. demonstrated that inclusion of the third TMT joint significantly altered the kinematics of adjacent joints and highlighted the importance of carefully evaluating the indication for extending the fusion to this joint [19]. The findings of the present study are consistent with and support this recommendation.

We observed minimal changes in JRF at the first metatarsophalangeal joint following TMT arthrodesis. Previous studies have reported conflicting findings: while one study demonstrated a 25% increase in first metatarsophalangeal joint dorsiflexion following first TMT joint arthrodesis [21], Kim et al. did not observe a similar effect [19]. When evaluating JRFs at the first metatarsophalangeal joint, our results are more consistent with those reported by Kim et al. Nevertheless, increased plantar pressure was observed in the first and second metatarsophalangeal joint regions in all models except Model II, particularly during the midstance and late-stance phases. These findings suggest that TMT arthrodesis may influence plantar pressure distribution even in the absence of substantial changes in joint reaction forces at the metatarsophalangeal level, and this potential effect should not be overlooked.

Analysis of plantar pressure revealed that the greatest increases occurred at the first and second metatarsophalangeal joint level, measuring approximately 20–30 kPa during midstance and 50–60 kPa during late stance. Previous studies have reported the minimal detectable change in plantar pressure in clinical settings to range between 30 and 80 kPa [39], while a threshold of approximately 200 kPa has been adopted in many studies as clinically relevant [40]. In the present study, none of the observed pressure changes reached these established thresholds. Nevertheless, forefoot ulceration following midfoot arthrodesis has been previously reported [41]. Therefore, awareness of potential alterations in plantar pressure remains particularly important, especially in high-risk patient populations such as individuals with diabetes mellitus.

The study is not without limitations. First, as the findings are derived from computational analyses, they are inherently based on modeling assumptions. Consequently, real-life clinical conditions may differ due to numerous patient- and case-specific factors. In addition, only a single CT-based model obtained from a healthy individual was used for the finite element analyses. Given that the clinical relevance of TMT arthrodesis is most pronounced in conditions such as hallux valgus and Lisfranc injuries, the use of models incorporating pathological anatomy might yield different biomechanical results. The use of a neutral, non-pathological foot model represents a simplification that facilitates comparative biomechanical analysis. Therefore, the findings should be interpreted as mechanistic insights rather than direct simulations of specific pathological conditions such as hallux valgus or Lisfranc injury. Bone tissue was modeled as a homogeneous structure with uniform material properties. While this approach facilitated simplification of the analyses, it should be noted that cortical and trabecular bone possess distinct mechanical characteristics, which were not differentiated in the present model. Similar simplifications were applied to the modeling of arthrodesis. Joint fusions were not simulated using fixation hardware; instead, the corresponding articular surfaces were fully bonded through contact definitions within the finite element framework. This represents a deliberate modeling choice and constitutes a limitation of the study, as the analysis was designed to investigate construct-specific biomechanical behavior following successful fusion rather than to simulate fixation stability or early postoperative mechanics. In clinical arthrodesis procedures performed with screws or plates, subtle differences in joint rigidity, degrees of freedom, and force transmission may occur. This modeling approach also precluded evaluation of the effects of different fixation materials on overall foot biomechanics. Finally, all fusion models were created without introducing any changes in alignment, preserving the native anatomical position. While this strategy allowed for direct comparison among different arthrodesis configurations, it does not fully reflect clinical practice, where corrective procedures that alter alignment are frequently performed in conjunction with fusion. Accordingly, the biomechanical consequences observed in this study should be interpreted within the context of these modeling constraints.

5. Conclusion

This finite element study demonstrates that the biomechanical consequences of tarsometatarsal arthrodesis depend on the extent of fusion. The most pronounced changes were observed at the medial–intermediate intercuneiform and calcaneocuboid joints, particularly with extension of fusion to the third tarsometatarsal joint. Accordingly, load redistribution following tarsometatarsal arthrodesis is strongly influenced by the extent of fusion.

Informed consent

Written informed consent was obtained from the individual whose computed tomography data were used for model generation and analysis.

Ethics approval and consent to participate

No ethical approval or consent was required, as this study did not involve human participants or animal experimentation.

Funding

This research received no specific grant from any funding agency in the, public, commercial, or not-for-profit sectors.

Data availability

Data of the study are available from the corresponding author on reasonable request.

Declaration of Competing Interest

The authors declare that they have no known competing financial interests or personal relationships that could have appeared to influence the work reported in this paper.

Acknowledgements

Not applicable.

Appendix A. Supporting information

Supplementary data associated with this article can be found in the online version at doi:10.1016/j.fas.2026.02.005.

References

[1] Lau SC, Guest C, Hall M, Tacey M, Joseph S, Oppy A. Do columns or sagittal displacement matter in the assessment and management of Lisfranc fracture dislocation? An alternate approach to classification of the Lisfranc injury. Injury 2017;48(7):1689–95. https://doi.org/10.1016/j.injury.2017.03.046
[2] Wong DWC, Zhang M, Yu J, Leung AKL. Biomechanics of first ray hypermobility: An investigation on joint force during walking using finite element analysis. Med Eng Phys 2014;36(11):1388–93. https://doi.org/10.1016/j.medengphy.2014.03.0041
[3] Morton DJ. Hypermobility of the first metatarsal bone: the interlinking factor between metatarsalgia and longitudinal arch strains. J Bone Jt Surg 1928;10(2):187–96.
[4] Symeonidis PD, Anderson JG. Original and modified lapidus procedures. J Bone Jt Surg Am 2021;103(4):e15. https://doi.org/10.2106/JBJS.20.010101
[5] Scheele CB, Kinast C, Lenze F, Wimmer J, Beischl S, Harrasser N. Radiographic evaluation of first tarsometatarsal joint arthrodesis for hallux valgus deformity: does the fusion of the first to the second metatarsal base reduce the radiological recurrence rate? Foot Ankle Spec 2024;17(4):382–90. https://doi.org/10.1177/193864002311642091
[6] Chopra S, Moerenhout K, Crevoisier X. Subjective versus objective assessment in early clinical outcome of modified Lapidus procedure for hallux valgus deformity. Clin Biomech 2016;32:187–93. https://doi.org/10.1016/j.clinbiomech.2015.11.0121
[7] So E, Van Dyke B, McGann MR, Brandao R, Larson D, Hyer CF. Structures at risk from an intermetatarsal screw for lapidus bunionectomy: a cadaveric study. J Foot Ankle Surg 2019;58(1):62–5. https://doi.org/10.1053/j.jfas.2018.08.0101
[8] Henning JA, Jones CB, Sietsema DL, Bohay DR, Anderson JG. Open reduction internal fixation versus primary arthrodesis for lisfranc injuries: a prospective randomized study. Foot Ankle Int 2009;30(10):913–22. https://doi.org/10.3113/FAI.2009.09131
[9] Feldman MW, Fucaloro S, Krivicich L, Kent S, Salzler MJ. Studies directly comparing Lisfranc injuries treated with primary arthrodesis or open reduction and internal fixation show no significant difference in return to sport and complications: A systematic review and meta-analysis. J Foot Ankle Surg 2025;64(3):318–27. https://doi.org/10.1053/j.jfas.2025.02.0051
[10] Levy CJ, Yatsonsky D, Moral MZ, Liu J, Ebraheim NA. Arthrodesis or open reduction internal fixation for lisfranc injuries: a meta-analysis. Foot Ankle Spec 2022;15(2):179–84. https://doi.org/10.1177/19386400209714191
[11] Cardoso DV, Veljkovic A. General considerations about foot and ankle arthrodesis. Any way to improve our results? Foot Ankle Clin 2022;27(4):701–22. https://doi.org/10.1016/j.fcl.2022.08.0071.1
[12] Gaedke IE, Wiebking U, O'Loughlin PF, Krettek C, Gaulke R. Clinical and radiological mid- to long-term outcomes following ankle fusion. Vivo 2018;32(6):1463–71. https://doi.org/10.21873/invivo.114001
[13] Willems A, Minnaard M, Oei EHG, Bierma-Zeinstra SMA, Meuffels DE. Talocrural arthrodesis increases osteoarthritis severity in adjacent joints: a midterm computed tomography follow-up study. Foot Ankle Spec 2025;18(5):548–55. https://doi.org/10.1177/193864002312085331
[14] Joveniaux P, Harisboure A, Ohl X, Dehoux E. Long-term results of in situ subtalar arthrodesis. Int Orthop (SICOT) 2010;34(8):1199–205. https://doi.org/10.1007/s00264-010-1041-51
[15] Smith RW, Shen W, Dewitt S, Reischl SF. Triple arthrodesis in adults with non-paralytic disease: a minimum ten-year follow-up study. J Bone Jt Surg Am 2004;86(12):2707–13. https://doi.org/10.2106/00004623-200412000-000181
[16] Sturnick DR, Demetracopoulos CA, Ellis SJ, Queen RM, Kolstov JCB, Deland JT, et al. Adjacent joint kinematics after ankle arthrodesis during cadaveric gait simulation. Foot Ankle Int 2017;38(11):1249–59. https://doi.org/10.1177/107110071772680611
[17] Nadaud JP, Parks BG, Schon LC. Plantar and calcaneocuboid joint pressure after isolated medial column fusion versus medial and lateral column fusion: a biomechanical study. Foot Ankle Int 2011;32(11):1069–74. https://doi.org/10.3113/FAI.2011.1069
[18] Wu G, Gu S, Yu G, Yin F. Effect of different fusion types on kinematics of midfoot lateral column: a comparative biomechanical study. Ann Transl Med 2019;7(22). https://doi.org/10.21037/atm.2019.10.21. 665-665.
[19] Kim J, Hoffman J, Steineman B, Eble SK, Roberts LE, Ellis SJ, et al. Kinematic analysis of sequential partial-midfoot arthrodesis in simulated gait cadaver model. Foot Ankle Int 2022;43(12):1587–94. https://doi.org/10.1177/107110072211252261
[20] Wang Y, Li Z, Zhang M. Biomechanical study of tarsometatarsal joint fusion using finite element analysis. Med Eng Phys 2014;36(11):1394–400. https://doi.org/10.1016/j.medengphy.2014.03.0141
[21] Perez MT, Owen JR, Adelaar RS, Wayne JS. Computational analysis of Lisfranc surgical repairs. J Orthop Res 2022;40(12):2856–64. https://doi.org/10.1002/jor.253081
[22] Liu Y, Lu W, Liu W, Wu W sheng, Wang C wei. Biomechanical analysis of elastic fixation for lisfranc injuries with finite elements method. Sci Rep 2025;15(1):26540. https://doi.org/10.1038/s41598-025-11611-91
[23] Olçar HA, Özer A, Mutu HB, Kuru T, Yurdakul G, Aydın D, et al. The biomechanical analysis of first metatarsocuneiform arthrodesis using the finite element method: A comparison of plate osteosynthesis in different positions. Ann Clin Anal Med 2024;15(04). https://doi.org/10.4328/ACAM.22077
[24] Cheung JT, Zhang M. A 3-dimensional finite element model of the human foot and ankle for insole design. Arch Phys Med Rehabil 2005;86(2):353–8.
[25] Yu J, Cheung JT, Wong DW, Cong Y, Zhang M. Biomechanical simulation of high-heeled shoe donning and walking. J Biomech 2013;46(12):2067–74.
[26] Tao K, Ji WT, Wang DM, Wang CT, Wang X. Relative contributions of plantar fascia and ligaments on the arch static stability: a finite element study. Biomed Tech 2010;55(5):265–71.
[27] Akrami M, Qian Z, Zou Z, Howard D, Nester CJ, Ren L. Subject-specific finite element modelling of the human foot complex during walking: sensitivity analysis of material properties, boundary and loading conditions. Biomech Model Mechanobiol 2018;17(2):559–76.
[28] Delp SL, Anderson FC, Arnold AS, Loan P, Habib A, John CT, et al. OpenSim: open-source software to create and analyze dynamic simulations of movement. IEEE Trans Biomed Eng 2007;54(11):1940–50.
[29] Haraguchi N, Armiger RS, Myerson MS, Campbell JT, Chao EY. Prediction of three-dimensional contact stress and ligament tension in the ankle during stance determined from computational modeling. Foot Ankle Int 2009;30(2):177–85.
[30] Zhu Y, Li X, Xu X. Ankle joint pressure change in varus malalignment of the tibia. BMC Musculoskelet Disord 2020;21(1):148. https://doi.org/10.1186/s12891-020-3163-21
[31] Yi Y, Chaudhari S. Various flexible fixation techniques using suture button for ligamentous lisfranc injuries: a review of surgical options. Medicina 2023;59(6):1134. https://doi.org/10.3390/medicina590611341
[32] Perkins JM, Vacketta VG, Brandão RA, Prissel MA, Hyer CF. Depth variations of second and third tarsometatarsal joints during dorsal compression staple fixation using two different bridge lengths: an anatomic study. Foot Ankle Surg Tech Rep Cases 2024;4(1):100353. https://doi.org/10.1016/j.fastrc.2023.100353
[33] Kim Y, Kim J, Lee KM, Koo S. The increase of joint contact forces in foot joints with simulated subtalar fusion in healthy subjects. Gait Posture 2019;74:27–32. https://doi.org/10.1016/j.gaitpost.2019.07.3761.1
[34] Kimura T, Kubota M, Suzuki N, Hattori A, Marumo K. Comparison of intercuneiform 1-2 joint mobility between hallux valgus and normal feet using weightbearing computed tomography and 3-dimensional analysis. Foot Ankle Int 2018;39(3):355–60. https://doi.org/10.1177/10711007177441741
[35] Kim J, El Masry S, Srikumar S, Palma J, Ellis S, Conti M. Association between postoperative medial-middle intercuneiform joint widening and recurrence rates in hallux valgus treated with modified lapidus procedure. Foot Ankle Int 2024;45(12):1349–58. https://doi.org/10.1177/107110072412868901

[36] Dugarte A, Bharwani S, Yoo H, Boiwka AV, Yu CC, Bajwa NS, et al. Calcaneocuboid joint arthritis of the midfoot precedes tibiotalar joint arthritis. Orthopedics 2016;39(6). https://doi.org/10.3928/01477447-20160819-04

[37] Ayala AE, Khwaja A, Goodison BC, Smith SL, Kim SY, Irwın JT, et al. Effect of fibular malrotation on tibiotalar joint contact mechanics in a Weber B ankle fracture model. Foot Ankle Spec 2024;17(6):577–84. https://doi.org/10.1177/193864002211278351

[38] Peiffer M, Lewis L, Xie K, Guild TT, Ashkani-Esfahani S, Kwon JY. The influence of talar displacement on articular contact mechanics: a 3D finite element analysis study using weightbearing computed tomography. Foot Ankle Int 2024;45(4):393–405. https://doi.org/10.1177/107110072412271791

[39] Rome K, Survepalli DG, Lobo M, Dalbeth N, McQueen F, McNair PJ. Evaluating intratester reliability of manual masking of plantar pressure measurements associated with chronic gout. J Am Podiatr Med Assoc 2011;101(5):424–9. https://doi.org/10.7547/10104241

[40] Castro-Martins P, Marques A, Coelho L, Vaz M, Costa JT. Plantar pressure thresholds as a strategy to prevent diabetic foot ulcers: a systematic review. Heliyon 2024;10(4):e26161. https://doi.org/10.1016/j.heliyon.2024.e26161

[41] Birke JA, Franks BD, Foto JG. First ray joint limitation, pressure, and ulceration of the first metatarsal head in diabetes mellitus. Foot Ankle Int 1995;16(5):277–84. https://doi.org/10.1177/107110079501600506

[42] Fedorov A, Beichel R, Kalpathy-Cramer J, Finet J, Fillion-Robin JC, Pujol S, et al. 3D slicer as an image computing platform for the quantitative imaging network. Magn Reson Imaging 2012;30(9):1323–41.

[43] Wu G, Siegler S, Allard P, Kirtley C, Leardini A, Rosenbaum D, et al. ISB recommendation on definitions of joint coordinate system of various joints for the reporting of human joint motion–part I: ankle, hip, and spine. International Society of Biomechanics. J Biomech 2002;35(4):543–8.

[44] Beumer A, van Hemert WL, Swierstra BA, Jasper LE, Belkoff SM. A biomechanical evaluation of the tibiofibular and tibiotalar ligaments of the ankle. Foot Ankle Int 2003;24(5):426–9.

[45] Marchetti DC, Moatshe G, Phelps BM, Dahl KD, Ferrari MB, Chahla J, et al. The proximal tibiofibular joint: a biomechanical analysis of the anterior and posterior ligamentous complexes. Am J Sports Med 2017;45(8):1888–92.

[46] Mercan N, Yurteri A, Dere Y. Do lateral ankle ligaments contribute to syndesmotic stability: a finite element analysis study. Comput Methods Biomech Biomed Eng 2024;27(13):1768–80.

[47] Li Y, Tong J, Wang H, Ji X, Hua Y, Cheng CK. Investigation into the effect of deltoid ligament injury on rotational ankle instability using a three-dimensional ankle finite element model. Front Bioeng Biotechnol 2024;12:1386401.

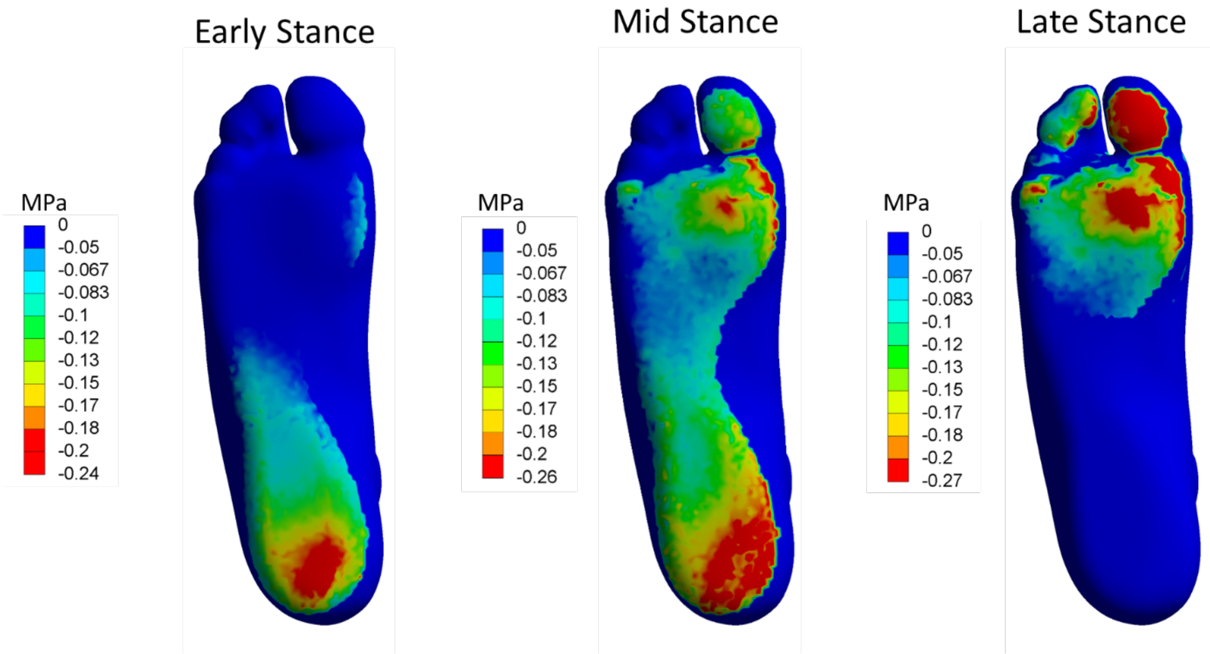

Supplementary Figure S6. Plantar pressure distributions of the intact model for the three phases of gait.

Previous computational analyses employing flat insole materials have reported peak plantar pressures between 0.214 and 0.266 MPa [24]. Furthermore, phase-specific plantar pressure values documented in both experimental and numerical studies typically range around 0.18 MPa for early stance, 0.21 MPa for midstance, and 0.22 MPa for late stance [27]. In the current analysis, the predicted peak plantar pressures across the gait cycle were found to be 0.236–0.265 MPa.

Reference

[48] Zhang L., Zhang Q., Zhong Y., Hortobagyi T., Gu Y. Effect of forefoot transverse arch stiffness on foot biomechanical response--based on finite element method. Front Bioeng Biotechnol 2024;12:1387768.1.